A lattice dynamics study of a Langmuir monolayer of monounsaturated fatty acids

Yehudi K. Levine
Department of Molecular Biophysics, Buys ballot Laboratory, University of Utrecht, P.O. Box 80.000, 3508 TA, Utrecht, The Netherlands

Andrzej Kolinski[a] and Jeffrey Skolnick
Department of Molecular Biology, The Scripps Research Institute, La Jolla, California 92037-1093

(Received 8 September 1992; accepted 27 January 1993)

A Monte Carlo dynamics (MCD) scheme has been applied in a study of the effects of unsaturated double bonds on the internal conformational dynamics and orientational order of hydrocarbon chains arranged in a monolayer on the surface of an impenetrable interface. The MCD algorithm makes use of the high coordination {2 1 0} lattice for the representation of both sp^3 and sp^2 valence states of the carbon atoms. The chain dynamics are considered to arise from a superposition of local conformational rearrangements. The simulations reproduced the principal features of the experimentally observed order parameter profiles of the C–H bonds on taking into account the intramolecular conformational energy of the molecules and excluded volume effects. The results show that the introduction of a rigid, planar, unsaturated segment enhances the orientational order in the monolayer. The extent of the enhancement is larger for the *trans* unsaturated chains than for the *cis* unsaturated ones. The increase in orientational order is accompanied by a marked increase in the effective rotational correlation times, indicating that the unsaturated segments undergo slow and restricted motion. In addition, the C–H bonds of the saturated chain segment between the *cis* double bond and the headgroup of the chain undergo slower motions than the corresponding vectors in the saturated and *trans* unsaturated chains. This arises from the anchoring of the headgroup at the impenetrable monolayer interface.

I. INTRODUCTION

The characterization of the orientational and motional properties of hydrocarbon chains in lipid bilayer systems has been the subject of many experimental and theoretical investigations.[1–4] A lipid bilayer is conveniently described as a back-to-back superposition of two monomolecular layers and indeed monolayers of lipid molecules at an air–water interface are often used to mimic the bilayer behavior. Despite much research efforts, the understanding of physical experiments in terms of the of the behavior of the hydrocarbon chains on a microscopic scale is still incomplete. The description of the orientational order and dynamics is impeded by factors such as the multiplicity of internal conformational motions and the implicit model dependence of the interpretation of the experiments. In particular, the effect of the introduction of unsaturated double bonds on the order and dynamics of the chains is still a subject of much debate.

A greater insight into the dynamics of hydrocarbon chains and the effects of unsaturation on their motional properties, is only possible through the interpretation of the experimental data with computer simulations of chain dynamics.[5–13] We have recently shown that the technique of Monte Carlo dynamics (MCD) provides a useful and efficient approach for simulating the conformational motions of saturated and unsaturated hydrocarbon chains.[14,15] The computational efficiency of the algorithm is achieved by performing the simulations on a lattice which permits the use of fast integer arithmetic operations. An added advantage is the simplicity and rigor of the implementation of excluded volume effects. The underlying assumption of the method is that the conformational dynamics can be described as a superposition of local structural rearrangements involving the transfer of methylene groups to different lattice sites.

The main drawback of the MCD method is the use of a lattice representation for the hydrocarbon chain. While the diamond lattice provides a faithful representation of the rotational isomeric states of an alkane chain, it cannot reproduce the planar configuration of *cis* or *trans* unsaturated double bonds, Fig. 1. This is merely a reflection of the different coordinations of the sp^3 and sp^3 valence states of the carbon atoms. On the other hand, both the tetrahedral and planar configurations can be reproduced on the high coordination {2 1 0} lattice.

Nevertheless, we have shown recently that the MCD algorithm based on the {2 1 0} lattice reproduces the chain dynamics for isolated hydrocarbon chains found from Brownian dynamics simulations.[14,15] In particular it was found that the measure of time used in the MCD simulation scales linearly with the real time of BD algorithms. This validation of the MCD scheme indicates its usefulness for the study of multichain dense systems, for which BD simulations would require unrealistically long computational times.

[a]Permanent address: Department of Chemistry, University of Warsaw, Pasteura 1, 02-093 Warsaw, Poland.

 0021-9606/93/097581-07$06.00

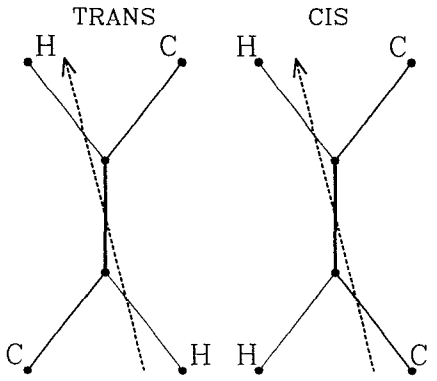

FIG. 1. The planar conformation of *trans* and *cis* double bonds. The dashed arrows show schematically the axes of orientation of the unsaturated segments in the monolayer. Note that the C–H bonds of the *cis* segment have different orientation to the axis, while the parallel C–H bonds of the *trans* segment have an equivalent orientation.

Here we present a MCD study of the effects of unsaturated double bonds on the internal conformational dynamics of hydrocarbon chains arranged in a monolayer on the surface of an impenetrable interface. Only the intramolecular conformational energy of the molecules and excluded volume effects entered the algorithm. The simulations reproduced the principal features of the experimentally observed order parameter profiles of the C–H bonds. Moreover they show that the introduction of a rigid, planar, unsaturated segment enhances the orientational order in the monolayer. The extent of the enhancement is larger for the *trans* unsaturated chains than for the *cis* unsaturated ones. The increase in orientational order is accompanied by a marked increase in the effective rotational correlation times, indicating that the unsaturated segments undergo slow and restricted motion. In addition, the C–H bonds of the saturated chain segment between the *cis* double bond and the headgroup of the chain undergo slower motions than the corresponding vectors in the saturated and *trans* unsaturated chains. This arises from the anchoring of the headgroup at the impenetrable monolayer interface.

II. METHOD OF SIMULATION

A. Geometric representation on a lattice

The representation of the hydrocarbon chain on a cubic lattice was discussed in detail previously[14,15] and will only be summarized here. The model hydrocarbon chain consists of N beads connected by N-1 bonds each of length $\sqrt{5}$ lattice units. The bonds are obtained by a permutation of the 24 vectors of the type $\{\pm 2, \pm 1, 0\}$. The bond vectors are chosen from this basis set so that the distance $R13$ between beads i and $i+2$ lies in the interval $\sqrt{10} \leqslant R13 \leqslant \sqrt{18}$. The torsional potential $U(\Phi)$ for the rotation about the sp^3–sp^3 bonds in the model chain is represented by symmetric square wells corresponding to the trans ($\Phi \approx 0$) and two *gauche* states (g^+ and g^-). Each of the effective trans and the two *gauche* wells contains the same number of dihedral states. The depth of the wells corresponding to the *gauche* states and the height of the barriers between them are chosen so as to reproduce the values of $\langle \cos \Phi \rangle$ and $\langle \cos^2 \Phi \rangle$ obtained from the continuous torsional potential for polymethylene chains over the temperature range 200–800 K. This ensures that the end-to-end distances of the model chains correspond closely to those of real polymethylene chains. The potential parameters are shown in Table I.

TABLE I. Square-well potentials for the rotation about a bond in the model chain.

Torsional angle	Energy (K)
sp^3–sp^3	
$155 < \lvert\Phi\rvert < 180$	1815.0
$90 < \lvert\Phi\rvert < 155$	280.0
$30 < \lvert\Phi\rvert < 90$	700.0
$0 < \lvert\Phi\rvert < 30$	0.0
sp^3–sp^2	
$155 < \lvert\Phi\rvert < 180$	366.0
$90 < \lvert\Phi\rvert < 155$	660.0
$30 < \lvert\Phi\rvert < 90$	0.0
$0 < \lvert\Phi\rvert < 30$	415.0

Excluded volume effects were implemented by surrounding each bead by 12 occupied lattice sites, forming an FCC envelope about its position. These sites were obtained from the cyclic permutation of the vectors $\{\pm 1, \pm 1, 0\}$. The first bead of the chain, however, was given a larger excluded volume envelope to model the larger volume of a carboxyl group of a fatty acid chain. The first bead at site $\{X,Y,Z\}$ was surrounded with an additional 16 occupied lattice sites at positions $\{X \pm 2, Y \pm 2, Z\}$, $\{X \pm 2, Y \pm 2, Z-1\}$, $\{X \pm 2, Y, Z\}$, $\{X \pm 2, Y, Z-1\}$, $\{X, Y \pm 2, Z\}$, and $\{X, Y \pm 2, Z-1\}$. With this enlarged envelope we were able to reproduce marked increase in the order parameter profile observed in the headgroup region of bilayers of fatty acids and lipids.[16,17] A smaller envelope for the first bead yields a parabolic profile characteristic of that observed for alcohol molecules in bilayers of ternary soap systems.[16]

The representation of the *cis* and *trans* double bond segments, Fig. 1, on the lattice was chosen so as to reproduce their rigid planar configuration. Forty-eight distinct triplet vector combinations taken from the set $\{\pm 2, \pm 1, 0\}$ were found to satisfy this condition for the *cis* segment and 96 for the *trans*. The construction of the planar segments involved vector triplets for which $R13 = \sqrt{18}$ and $\sqrt{16}$.

The continuous torsional potential for rotation about the sp^3–sp^2 bond,[14,15] is represented by square wells as described above. The potential parameters used in the simulations are given in Table I.

B. Construction of a monolayer of model chains

The XY plane of the lattice was taken to represent the interface of the monolayer. The interface was impenetrable for the model chains as all the lattice sites in the half-space $Z < 0$ were permanently occupied during the simulations. The chains were attached to the interface with the first

bead of each one allowed to move vertically by one lattice unit, so that it occupied positions in the XY plane at heights $Z=1$ and $Z=2$.

The initial configuration of the monolayer was constructed as follows. Sixty-four model chains were confined into a Monte Carlo box having a square cross section in the XY plane and extending along the positive Z axis. Periodic boundary conditions applied throughout. The box at height $Z=1$ was divided into 8×8 square cells in the XY plane. The packing density of the chains was varied by changing the side of the cells. A random chain configuration was generated and fixed with its first bead at the centre of one of the cells. The cells were then filled sequentially with 63 identical chains. The monolayer configuration thus constructed was accepted only if every bead and its associated excluded volume envelope occupied distinct lattice sites. The monolayer was subsequently equilibrated at a particular temperature prior to the simulation run. The results of the simulations were found to be independent of the starting configuration of the monolayer system. Identical were also obtained for the same packing density using a rectangular MC box.

C. Conformational motions

The conformational dynamics of the model polymethylene chain is considered to arise from a superposition of local structural rearrangements constrained by the bond lengths. The elementary move involves the transfer of a pair of adjacent beads, –C1–C2–, chosen at random to different lattice sites.[15] As the chain segment –C1–C2– is uniquely characterized by the triplet of lattice vectors assigned to the bonds, the moves are described simply as random interchanges between vector triplets can be carried out efficiently by the use of a lookup table.[15]

The first and last bonds are allowed to undertake random orientations. The lack of restrictions on the positions of the first beads in the XY plane resulted in a lateral translational motion of the chains across that plane. The interaction of the headgroups of real chains with the water interface, was simulated by accepting a move of the first bead only once every 100 times it was picked. This value was chosen so as to make the time scale of the lateral diffusion of the chains an order of magnitude longer than that observed for the internal conformational motions. It is important to note that the precise value chosen does not affect the order parameter profile of the chains. Nevertheless, a higher frequency of acceptance of the moves for the first beads, was found to result not only in faster lateral diffusion, but also in internal conformational dynamics characteristic of chains with two free ends.

The local conformational moves for the polymethylene model chain in the vicinity of an unsaturated segment are formulated under the constraint that the four bead segment –C2–C3=C4–C5– forms a rigid entity as a result of the lack of rotational freedom about the double bond. Consequently the constituent beads, C2 to C5, can only be displaced to different lattice sites by a large scale collective move. It has been shown previously[15] that this is achieved most simply by the execution of the translationally asymmetric collective four bead move involving all beads of segments of the type –C1–C2–C3=C4– or –C3=C4–C5–C6– shown schematically in Fig. 2. The segments are uniquely characterized by the set of the five bond vectors and the random interchanges between the sets are again implemented simply using lookup tables.

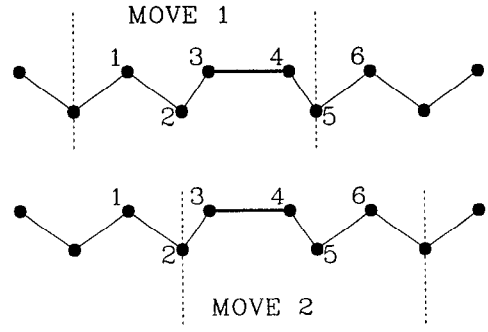

FIG. 2. The schematic representation of the lattice moves of the *cis* and *trans* unsaturated segments. The double bond is at the 3/4 position. The beads enclosed by the dashed vertical lines are moved to new lattice sites, leaving the other beads at the same position. Either move 1 or move 2 is carried out.

Each random elementary moves attempted by the beads are subjected to three acceptance tests:

(1) A move is only accepted if the final lattice positions of the beads are unoccupied. This applies to both a bead and its associated excluded volume envelope.

(2) The new configuration was accepted with a probability P given by the symmetric scheme

$$P=\exp(-E_{\text{new}}/kT)/\{\exp(-E_{\text{old}}/kT)+\exp(-E_{\text{new}}/kT)\}.$$

This test is convenient as it is determined by the differences in the torsional energy involved in the move, rather than by absolute values.

(3) Chain configurations with g^+g^- or g^-g^+ conformations about adjacent bonds are rejected. In the g conformation the torsional angle Φ lies in the range $155\leqslant|\Phi|\leqslant90$. This constraint, however, is not applied to the conformation about sp^3–sp^2 bonds adjacent to the unsaturated segment.

The Monte Carlo dynamics algorithm for a model chain consisting of N beads was executed in the following way. Given a particular configuration of the chain, Ω_j, N local conformational moves are attempted so that each bead having an equal chance of being picked. These N moves generate a new configuration of the chain, Ω_{j+1}. The cycle is now repeated using Ω_{j+1} as the starting configuration. The fundamental time step of the algorithm is defined as the time required for the chain to undergo a transition from configuration Ω_j to Ω_{j+1}. However this approach does not relate the time step to an absolute scale.

We have typically generated a trajectory consisting of $2\cdot10^4$ monolayer configurations each separated by 50 elementary time steps at a temperature of 350 K. The calculation for a monolayer of 64 chains each consisting of 18

beads required 18 h on a DEC3100 workstation. With this choice, the statistical fluctuations in the calculated average chain parameters obtained from runs starting with different initial conformations varied by less than 5%. Furthermore, the decay of the time-correlation functions for every bead of the chain was found to be independent of the interval between successive configurations along the trajectory generated. The only caveat being that the total time of the trajectory used for the evaluation of the correlation functions must be long compared to the decay time of the slowest decay component.

D. Analysis of the trajectories

The time autocorrelation function, $G_2(t)$, for motion of any chain vector,

$$G_2(t)=\langle\langle P_2\{\mu(0)\cdot\mu(t)\}\rangle\rangle \tag{1}$$

is obtained from the sequence of generated configurations, Ω_k's along the trajectory. The double brackets indicate an ensemble average over all 64 chains. The spatial orientation of the C–H vectors attached to any bead of the model chain can be defined uniquely from the bond vectors of the model chain.[15]

The rates of motion can be estimated from the correlation functions $G_2(t)$, by defining the generalized rotational correlation time τ, as

$$\tau=\frac{\int_0^\infty [G_2(t)-G_2(\infty)]dt}{G_2(0)-G_2(\infty)}, \tag{2}$$

where

$$G_2(\infty)=\langle P_2(\cos\beta)\rangle^2=S^2. \tag{3}$$

Here β denotes the angle between the vector and the lattice Z axis. We have evaluated τ by fitting the time-correlation functions to a multiexponential decay of the form

$$G_2(t)=\sum_m a_m \exp[-t/\phi_m]+G_2(\infty) \tag{4}$$

and the correlation time τ, Eq. (2) is now given by

$$\tau=\frac{\Sigma_m a_m\phi_m}{\Sigma_m a_m}. \tag{5}$$

It turned out in practice that the decay of the correlation functions $G_2(t)$ was best described using four exponential decay components.

III. RESULTS AND DISCUSSION

A. Equilibrium properties

The simulation runs were carried out for 18 bead saturated, *cis*- and *trans*-unsaturated chains in a square MC boxes with sides varying from 48 to 72 lattice units. Only excluded volume interactions and the conformational energy of the chains were considered here. The chains were found to be conformationally disordered at any given box size. This can be quite simply seen from the distribution of the height of the beads above the impenetrable XY plane shown in Fig. 3 for the 9/10 *cis* unsaturated chain in boxes with sides 48 and 72 lattice units.

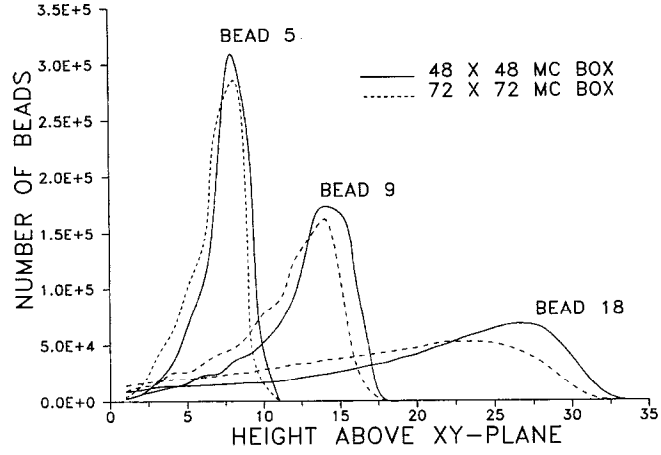

FIG. 3. The distributions of the positions of chain beads 5, 9, and 18 along the Z axis, the normal to the plane of the monolayer.

The widths of the distributions increase on moving down the chain from the interface to the free tail and interestingly, every bead in the chain was found to have a small probability of reaching the impenetrable interface. The chance of finding a bead at the interface is markedly greater for beads near the free tail than for those near the constrained headgroup. This finding suggests that the chains may form loops near their ends so that beads from the tail segments can fill lattice site vacancies near the monolayer plane. We note that the position of the maxima of the height distributions are found to shift towards the interface on increasing either size of the MC box in agreement with the observed shortening of the end-to-end distances of the chains.

Similar behavior was found for the saturated as well as the *trans* and *cis* unsaturated chains irrespective of the position of the double bond segment along the chain.

The extent of conformational disorder of the chains is monitored experimentally by ^{2}H-NMR on either perdeuterated or selectively deuterated molecules.[16] This is conveniently expressed in terms of the order parameter S, $S=1/2\langle 3\cos^2\beta-1\rangle$, where β denotes the angle between the C–D vector and the normal to the plane of the monolayer, here the **Z** axis. It now needs to be recognized that the C–D vector attached to a sp^3–sp^2 bond system lies in the plane defined by the two bond vectors, Fig. 1. On the other hand, the C–D vector in a saturated chain is oriented tetrahedrally relative to the plane defined by the sp^3–sp^3 bonds. The C–D bonds attached to each bead of the model saturated and unsaturated chains exhibited a uniform macroscopic orientational distribution in the **XY** plane within statistical error, thus indicating a uniaxial structure of the model monolayer.

The order parameter profile along the length of a 9/10 *cis* unsaturated chain in a MC box of side 60 lattice units at is shown in Fig. 4. It can be seen that the order parameters correspond closely to those observed experimentally for oleic acid chains incorporated into membranes of *acheo-*

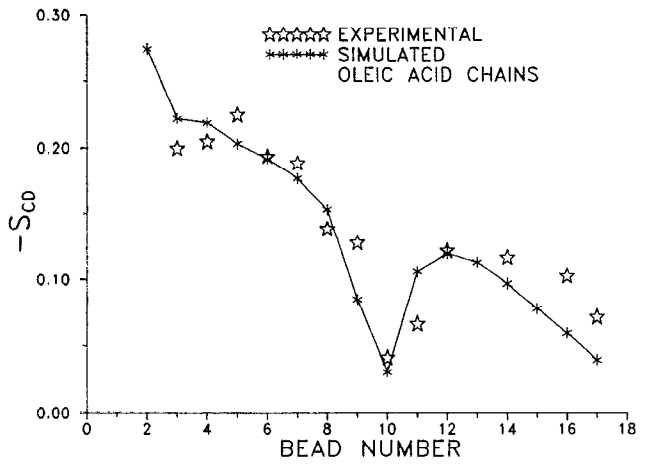

FIG. 4. A comparison of the order parameter profile of the C–D vectors of a model 9/10 *cis* unsaturated chains in a monolayer with experimental data obtained from NMR experiments on the same chains incorporated into a biological membrane.

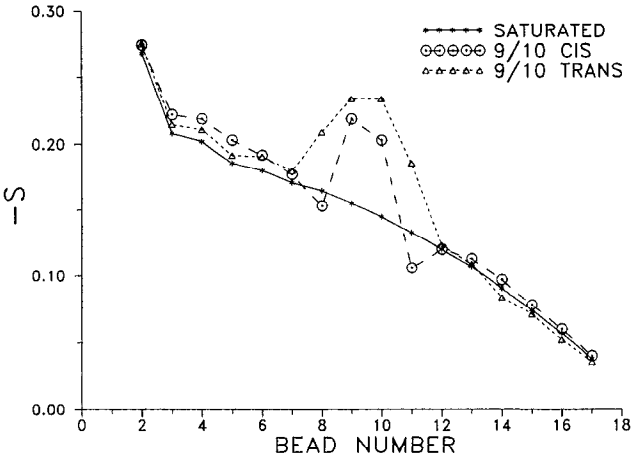

FIG. 5. The order parameter profile of tetrahedrally bonded C–D vectors of model chains in a square MC box of side 60 lattice units.

plasma lailawii.[18] In particular, the simulations reproduce the distinct minimum of the order parameter profile at the 10 position, Fig. 4. This dip is found to be characteristic of *cis* unsaturated chains, irrespective of the position of the double bond in the chain. The minimum is always found for the bead furthest from the headgroup. The observation of significantly different order parameters for the equivalent C–D vectors of a *cis* segment, has been previously attributed to the fact that the orientational axis of this segment does not coincide with the direction of the double bond itself, Fig. 1.[19,20]

The simulations show that the appearance of the order parameter dip has a simple geometric origin and arises from the preferential alignment of the double bond segment along the **Z** axis. This can be seen from the high order parameter, $S=0.39$ found for the 9/10 bond. It is interesting to note that a value of 0.37 for this order parameter was obtained from infrared dichroism experiments on egg–lecithin bilayers.[21] The order parameter, $S=-0.29$, found for the normal to the plane of the *cis* segment shows that the plane of the unsaturated segment is well aligned along the **Z** axis. As the C–D bonds make an angle of 60° to the double bond, Fig. 1, this results in a low value for their order parameter S.

The simulations clearly indicate that the introduction of a planar and rigid unsaturated segment enhances the degree of orientational order in its vicinity, rather than produces a disruptive effect. This enhancement of the orientational order along the normal to the monolayer plane can be seen from a comparison of the order parameter profiles of C–D bonds in the saturated and unsaturated model chains constrained in the same MC box. However, in order to carry out such a comparison, we need to consider vectors having the same direction in the plane defined by the two backbone bonds of each bead. This is achieved most conveniently by considering C–D vectors attached at the tetrahedral angle to every bead of the model chains.

The saturated chains, Fig. 5, exhibit a monotonically decreasing order parameter profile in agreement with experiments.[16,17] It can be seen quite clearly that the order parameters of these vectors are significantly higher for the *cis* unsaturated than for the saturated chain at the position of the unsaturated segment. This is reflected in the lower value of order parameter found for the 9/10 bond vector in the saturated chain, $S=0.17$, compared to that, $S=0.39$, for the same vector in the 9/10 *cis* unsaturated chain. Interestingly, the C–D vectors attached to beads 8 and 11, the nearest neighbors to the double bond exhibit somewhat lower order parameters than the corresponding vectors in the saturated chain. This is a simple geometric consequence of fitting the rigid *cis* unsaturated segment, Fig. 1, into a polymethylene chain.

A similar behavior is found for chains containing unsaturated segments in different positions along the chain. The enhanced orientational order relative to the saturated chain is found to be more pronounced for unsaturated segments near the headgroup of the chain, than for segments near the free chain ends.

Figure 5 also shows the order parameter profile of tetrahedrally attached C–D bonds in a 9/10-*trans* unsaturated chain constrained in an MC box with side 60 lattice units. Interestingly, higher order parameters are found not only for the C–D bonds attached to beads 9 and 10, but also for their nearest neighbors, beads 8 and 11. We note that as the C–D bonds attached to the *trans* segment are parallel, they exhibit the same order parameter. The order parameter profile found here is again in good agreement with that obtained from ^{2}H-NMR experiments.[19,20]

The enhanced degree of orientational order is reflected in the high values of the order parameters, 0.36, 0.34, and 0.36 for the 8/9, 9/10, and 10/11 backbone vectors, respectively. Much lower values, 0.18, 0.17, and 0.16 are found for the corresponding vectors in the saturated chains. It appears therefore that the *trans* unsaturated segment has a more marked effect on the orientational order of the chain than a *cis* segment. Again, the unsaturated segment of the *trans* unsaturated chains exhibits a high

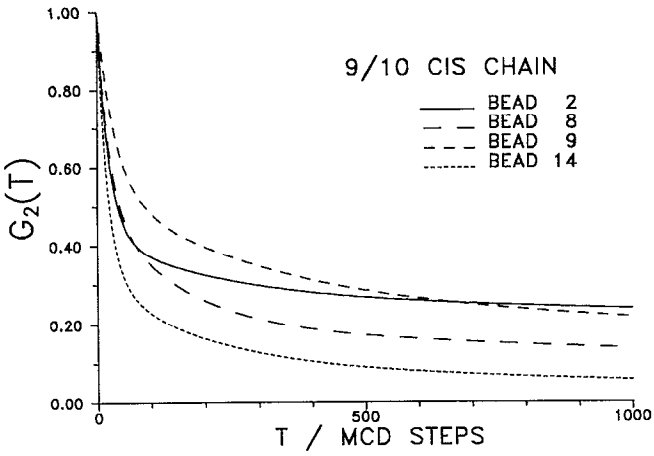

FIG. 6. The decay of the correlation function $G_2(t)$, Eq. (1) in the text, of the tetrahdral C–D vectors attached to beads 2, 8, 9, and 14 of the model 9/10 *cis* unsaturated chains in a MC box of side 60 lattice units. Note that the correlation function for bead 9 decays more slowly than that for the adjacent bead 8. The correlation functions decay to constant values corresponding to S^2, where S is the order parameter.

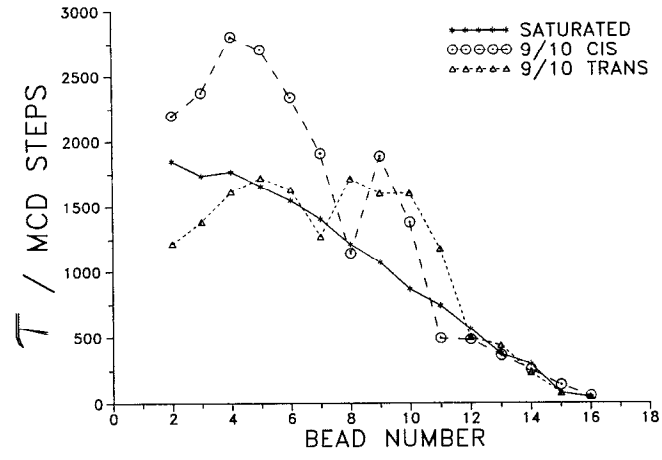

FIG. 8. The variation of the generalized correlation time τ of the terahderally bonded C–D along the length of the saturated, 9/10 *cis* and 9/10 *trans* unsaturated chains in a square MC box of side 60 lattice units. The time τ is defined by Eq. (2) in the text has been obtained from a fit of the decay of the correlation function to a four component exponential decay as given by Eq. (5) in the text.

degree of alignment along the **Z** axis, the normal to the monolayer plane.

Finally we note that an increase in the MC box size leads to an lowering of the order parameters in agreement with experiments.[16,17,22]

B. Dynamic properties

Typical decays of the time correlation function $G_2(t)$ for C–D vectors attached to beads 2, 8, 9, and 14 in 9/10 *cis* unsaturated and saturated chain confined to a square MC box of side 60 lattice units are shown in Figs. 6 and 7.

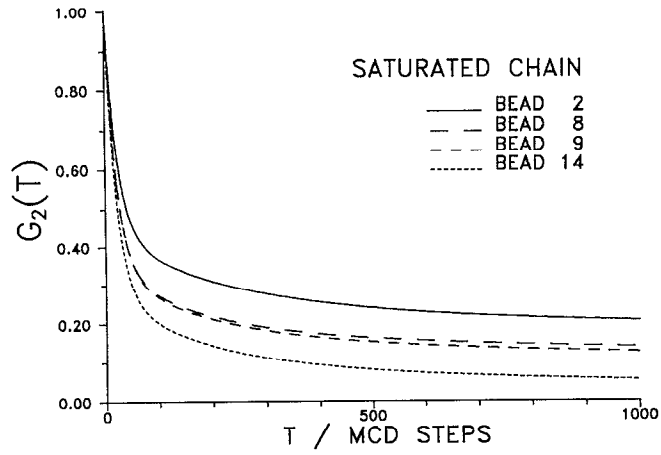

FIG. 7. The decay of the correlation function $G_2(t)$, Eq. (1) in the text, of the tetrahdral C–D vectors attached to beads 2, 8, 9, and 14 of the model saturated chains in a MC box of side 60 lattice units. Note that the correlation function for bead 9 exhibits a faster decay than that for the adjacent bead 8. This behavior is the opposite of that found for the same beads in the 9/10 *cis* unsaturated chain, Fig. 6. The correlation functions decay to constant values corresponding to S^2, where S is the order parameter.

Again for the sake of convenience we consider the vectors to be tetrahedrally bonded. The correlation functions decay to a constant plateau at long times whose height corresponds to the square of the equilibrium order parameter, S^2, within a 5% uncertainty limit. We implicitly assume here that that the measure of time in the Monte Carlo algorithm scales linearly with real time and furthermore is independent of the position along the model chain. This is justified by our previous finding[14,15] of a linear relation between the time used in BD algorithms and the MCD measure of time in isolated chains.

Figures 6 and 7 show clearly that the correlation function for the C–D vector attached to bead 9 of the *cis* unsaturated chain exhibits the slowest decay. Moreover, while the correlation function for the C–D vector attached to bead 8 in the *cis* unsaturated chain decays faster than that attached to bead 9, the opposite behavior is observed in the saturated chain. The same behavior is observed on increasing the of the MC box, though now the correlation functions decay more rapidly with a concomitant fall in the height of the long time plateaus. Similar effects are found for the 9/10 *trans* unsaturated chains.

The decay of the time correlation function for the C–D vectors attached to every bead of the chains was excellently described by the four component multiexponential decay, Eq. (4). The effective correlation time, τ, for the decay was obtained from Eq. (5). The values of the decay times of the exponential components, ϕ_m, for vectors in the middle of the saturated chain were typically of the order 20, 175, 1200, and 16000 MCD steps. The corresponding amplitudes were found to be 0.65, 0.16, 0.07, and 0.07.

The variation of the effective correlation times, Eq. (5), along the length of the chain is shown in Fig. 8 for the saturated, 9/10 *cis* and 9/10 *trans* unsaturated chains. The correlation time for bead 17 was too short to be determined accurately and has been omitted. The general form of the

decrease of τ along the length of the chain is in good agreement with ^{2}H-NMR relaxation time measurements in saturated lipid bilayers.[17,23–25] The reduction in the value of τ for the C–D vectors near the free ends of all three types of chain arises from a general decrease in the value of the decay times of all four exponential components. The high values of τ found at the position of the double bond in the unsaturated chains are due to the increase in the decay times of all four exponential components.

The most pronounced difference between the dynamics of the model saturated and unsaturated chains is found at the position of the double bond segment, Fig. 8. While the correlation times of the C–D bonds attached to beads 9 and 10 of the *cis* unsaturated chain are considerably larger than those attached to a saturated chain, the slowdown in dynamics extends over four beads, 8 to 11, for the *trans* unsaturated chain. A similar behavior has been found for the dynamics of isolated chains.[15] The finding of markedly slower reorientational motions in *cis* unsaturated chains relative to saturated ones is corroborated by the results of ^{2}H-NMR relation time measurements on lipid bilayers.[23,24]

Figure 8 shows that the introduction of a *cis* double bond induces a marked slow down in the conformational motions of the saturated chain segment between the double bond and the headgroup of the chain. This slowdown is reflected in every exponential decay components describing the decay of the correlation function, Eq. (4). On the other hand, a slight decrease in the correlation time is induced by the introduction of a *trans* bond.

The increase in the correlation times for the C–D vectors in the model *cis* unsaturated chains relative to those in the saturated chain is in marked contrast to the behavior reported previously for isolated chains with two free ends.[15] Nevertheless, a marked relative slowdown in the dynamics of an isolated *cis* unsaturated model chain is observed on constraining the first bead of the chains to move over the surface of a cube of side 2 lattice units. Furthermore, simulations of a monolayer containing a single chain reveal the same variation of the effective correlation time over its length as shown in Fig. 8 for both the *cis* unsaturated and saturated chains. The correlation times found for the case of a single chain are a factor 5–6 times shorter than those found for the chains in the monolayer. Similarly, the differences in the dynamic behavior between the saturated chain and the *trans* unsaturated again arise from the anchoring of the first bead. Importantly, the bias applied to the frequency with which the first bead is picked has only a small effect on the relative values of the correlation times for the beads in all three types of model chains. It thus appears that the dynamic profile of the chains reported here is determined by both the packing of the chains in the monolayer and their anchoring to the impenetrable monolayer surface.

IV. CONCLUSIONS

Monte Carlo dynamics simulations of supported monolayers of saturated and unsaturated chain molecules at a constant area have been carried out. The algorithms took account of the intramolecular conformational energy of the molecules and excluded volume effects only. These were found to be sufficient for reproducing the principal features of the experimentally observed order parameter profiles of the C–D bonds. The simulations show that the introduction of a rigid, planar, unsaturated segment enhances the orientational order in its vicinity rather than causes a disruptive effect. The extent of the enhancement is larger for the *trans* unsaturated chains than for the *cis* unsaturated ones. The increase in orientational order is accompanied by a marked increase in the effective rotational correlation times, indicating that the unsaturated segments undergo slow and restricted motion. In addition, the C–D bonds of the saturated chain segment between the *cis* double bond and the headgroup of the chain undergo slower motions than the corresponding vectors in the saturated and *trans* unsaturated chains. This arises from the anchoring of the headgroup at the impenetrable monolayer interface.

[1] G. Cevc and D. Marsh, *Phospholipid Bilayers: Physical Principles and Models* (Wiley-Interscience, New York, 1987).
[2] D. M. Small, *The Physical Chemistry of Lipids* (Plenum, New York, 1986).
[3] B. L. Silver, *The Physical Chemistry of Membranes* (Solomon, New York, 1985).
[4] M. D. Houslay and K. K. Stanley, *Dynamics of Biological Membranes* (Wiley, Chichester, 1982).
[5] K. A. Dill, J. Naghizadeh, and J. A. Marqusee, Annu. Rev. Phys. Chem. **39**, 425 (1988).
[6] R. W. Pastor, R. M. Venable, and M. Karplus, Proc. Natl. Acad. Sci. U.S.A. **88**, 892 (1991).
[7] A. Ferrarini, P. L. Nordio, G. J. Moro, R. H. Crepeau, and J. H. Freed, J. Chem. Phys. **91**, 5707 (1989).
[8] B. Egberts, W. F. van Gunsteren, and H. J. C. Berendsen, J. Chem. Phys. **89**, 3718 (1988).
[9] K. Watanabe and M. L. Klein, J. Phys. Chem. **93**, 6897 (1989).
[10] H. L. Scott and S. Kalaskar, Biochemistry **28**, 3687 (1989).
[11] R. W. Pastor, R. M. Venable, and M. Karplus, J. Chem. Phys. **89**, 1112 (1988).
[12] R. W. Pastor, R. M. Venable, M. Karplus, and A. Szabo, J. Chem. Phys. **89**, 1128 (1989).
[13] A. Rey, A. Kolinski, J. Skolnick, and Y. K. Levine, J. Chem. Phys. **97**, 1240 (1992).
[14] Y. K. Levine, Mol. Phys. **78**, 619 (1993).
[15] J. Seelig, Q. Rev. Biophys. **10**, 353 (1977).
[16] J. H. Davis, K. R. Jeffrey, and M. Bloom, J. Magn. Reson. **29**, 191 (1978).
[17] M. Rance, K. R. Jeffrey, A. P. Tulloch, K. W. Butler, and I. C. P. Smith, Biochim. Biophys. Acta **600**, 245 (1980).
[18] J. Seelig and N. Waespe-Sarcevic, Biochemistry **17**, 3310 (1978).
[19] A. Seelig and J. Seelig, Biochemistry **16**, 45 (1977).
[20] U. P. Fringeli, Z. Naturforsch. Tiel C **32**, 20 (1977).
[21] B. Mely, J. Charvolin, and P. Keller, Chem. Phys. Lipids **15**, 161 (1975).
[22] M. F. Brown, J. Seelig, and U. Häberlen, J. Chem. Phys. **70**, 5055 (1979).
[23] M. R. Paddy, F. W. Dalquist, E. A. Dratz, and A. J. Deese, Biochemistry **24**, 5988 (1985).
[24] M. F. Brown, A. A. Ribeiro, and G. D. Williams, Proc. Natl. Acad. Sci. U.S.A. **80**, 4325 (1983).